This article was downloaded by: [Renmin University of China]
On: 13 October 2013, At: 10:46
Publisher: Taylor & Francis
Informa Ltd Registered in England and Wales Registered Number: 1072954 Registered office: Mortimer House, 37-41 Mortimer Street, London W1T 3JH, UK

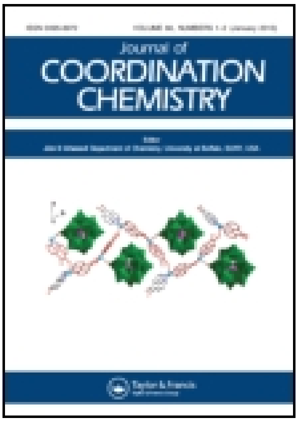

Journal of Coordination Chemistry
Publication details, including instructions for authors and subscription information:
http://www.tandfonline.com/loi/gcoo20

# Synthesis, structures, and fluorescence properties of two lanthanide [Ln=Sm(III), Nd(III)] coordination polymers

Lei Wang [a] & Liang Ni [a]

[a] School of Chemistry and Chemical Engineering , Jiangsu University , Zhenjiang 212013 , PR China

Published online: 02 Apr 2012.

To cite this article: Lei Wang & Liang Ni (2012) Synthesis, structures, and fluorescence properties of two lanthanide [Ln=Sm(III), Nd(III)] coordination polymers, Journal of Coordination Chemistry, 65:9, 1475-1483, DOI: 10.1080/00958972.2012.675433

To link to this article: http://dx.doi.org/10.1080/00958972.2012.675433

PLEASE SCROLL DOWN FOR ARTICLE

Taylor & Francis makes every effort to ensure the accuracy of all the information (the "Content") contained in the publications on our platform. However, Taylor & Francis, our agents, and our licensors make no representations or warranties whatsoever as to the accuracy, completeness, or suitability for any purpose of the Content. Any opinions and views expressed in this publication are the opinions and views of the authors, and are not the views of or endorsed by Taylor & Francis. The accuracy of the Content should not be relied upon and should be independently verified with primary sources of information. Taylor and Francis shall not be liable for any losses, actions, claims, proceedings, demands, costs, expenses, damages, and other liabilities whatsoever or howsoever caused arising directly or indirectly in connection with, in relation to or arising out of the use of the Content.

This article may be used for research, teaching, and private study purposes. Any substantial or systematic reproduction, redistribution, reselling, loan, sub-licensing, systematic supply, or distribution in any form to anyone is expressly forbidden. Terms & Conditions of access and use can be found at http://www.tandfonline.com/page/terms-and-conditions

*Journal of Coordination Chemistry*
Vol. 65, No. 9, 10 May 2012, 1475–1483

Taylor & Francis
Taylor & Francis Group

# Synthesis, structures, and fluorescence properties of two lanthanide [Ln = Sm(III), Nd(III)] coordination polymers

LEI WANG and LIANG NI*

School of Chemistry and Chemical Engineering, Jiangsu University,
Zhenjiang 212013, PR China

(*Received 3 November 2011; in final form 3 February 2012*)

Two three-strand coordination polymers $[Ln_2(m\text{-}BDC)_3(MOPIP)_2 \cdot H_2O]_n$ [Ln = Sm (**1**), Nd (**2**)] have been synthesized by hydrothermal reaction of lanthanide chloride with benzene-1, 3-dicarboxylic acid and 2-(4-methoxyphenyl)-1*H*-imidazo[4,5-f][1,10]phenanthroline (MOPIP). The crystal structures of the complexes are zipper-like chains of eight-coordinate $Ln^{3+}$, in which $Ln^{3+}$ ions are bridged in two coordination modes by $m\text{-}BDC^{2+}$ and decorated by MOPIP. The fluorescence property and thermal stability were also investigated.

*Keywords*: Lanthanides; Benzene-1,3-dicarboxylic acid; 2-(4-Methoxyphenyl)-1*H*-imidazo [4,5-f][1,10]phenanthroline; Crystal structure

## 1. Introduction

Lanthanide complexes are of great interest owing to various topological networks and crystal packing motifs as well as potential applications in fluorescent probes, magnetic materials, catalysts, and molecular sensors [1–4]. Geometries and properties of organic ligands exert great effect on structural frameworks of lanthanide complexes [5]. Thus much effort has been devoted to modify the building blocks and to control the assembled motifs for desired products through the selection of different ligands. 1,10-Phenanthroline (phen) and its derivatives are good candidates for construction of metal–organic supramolecular architectures through $\pi\cdots\pi$ interactions. In addition, strong absorptions within a large wavelength range for the $\pi \rightarrow \pi^*$ transition of phen are important, from which the energy can be effectively transferred to Ln(III) for intense emissions [6]. For example, photoluminescence measurements show that $[HNMe_2][Ln_2(m\text{-}BDC)_3(phen)_2]$ (Ln = Eu and Tb, $m\text{-}H_2BDC$ = 1,3-benzenedicarboxylic acid, phen = 1,10-phenanthroline) are highly emissive at room temperature and may be good candidates for light-emitting diodes and light applications [7]. In this contribution, we selected 2-(4-methoxyphenyl)-1*H*-imidazo[4,5-f][1,10]phenanthroline (MOPIP) as the neutral chelating ligand. Reports of this field are now maturing [8, 9].

---

*Corresponding author. Email: niliang@ujs.edu.cn

*Journal of Coordination Chemistry*
ISSN 0095-8972 print/ISSN 1029-0389 online © 2012 Taylor & Francis
http://dx.doi.org/10.1080/00958972.2012.675433

Lanthanides have high affinity for hard donors, and ligands with oxygen or hybrid oxygen–nitrogen atoms, especially multicarboxylate ligands, are usually employed in construction of lanthanide complexes. Benzene-1,3-dicarboxylic acid ($m$-$H_2BDC$) possesses intriguing coordination behavior and potential hydrogen-bond interactions, such as asymmetric geometry and multiple coordination sites.

By means of hydrothermal technique, two new lanthanide complexes $[Ln_2(m\text{-}BDC)_3(MOPIP)_2 \cdot H_2O]_n$ [Ln = Sm (**1**), Nd (**2**)] have been prepared with $m$-$H_2BDC$ and MOPIP ligands. The luminescence and thermal stability have also been investigated. From the luminescent property, the compound will be an excellent candidate for potential photoluminescent materials and is quite stable.

## 2. Experimental

### 2.1. *Materials and physical measurements*

MOPIP was synthesized according to the literature [8]. $Ln(Cl)_3 \cdot 6H_2O$ [Ln = Sm (**1**), Nd (**2**)], NaOH, and $m$-$H_2BDC$ were purchased commercially and used without purification. Transmission mode FT-IR spectra were obtained as KBr pellets between 4000 and 400 $cm^{-1}$ using a Nicolet Nexus 470 infrared spectrometer. Elemental analysis was carried out with a Perkin-Elmer 240C analyzer. Thermogravimetric analysis (TGA) was performed with a TA Instrument with a heating rate of 10°C $min^{-1}$ in air.

### 2.2. *Syntheses*

**2.2.1. $[Sm_2(m\text{-}BDC)_3(MOPIP)_2 \cdot H_2O]_n$ (1).** A mixture of $SmCl_3$ $6H_2O$ (0.183 g, 0.5 mmol), $m$-$H_2BDC$ (0.083 g, 0.5 mmol), MOPIP (0.163 g, 0.5 mmol), NaOH (0.004 g, 0.1 mmol), and $H_2O$ (18 mL) was placed in a 25 mL Teflon-lined stainless steel vessel under autogenous pressure at 165°C for 5 days. After cooling to room temperature, red block crystals of **1** were collected by filtration and washed with distilled water giving 60% yield (based on Ln). Anal. Calcd for **1** $C_{64}H_{42}N_8O_{15}Sm_2$ (%): C, 52.51; H, 2.89; N, 7.66. Found (%): C, 52.53; H, 2.87; N, 7.65. IR (KBr): $\acute{\upsilon} = 3381$(w), 1614(s), 1529(s), 1451(s), 1398(s), 1256(m), 1182(w), 1077(m), 741(m), 525(m), 423(m) $cm^{-1}$.

**2.2.2. $[Nd_2(m\text{-}BDC)_3(MOPIP)_2 \cdot H_2O]_n$ (2).** A mixture of $NdCl_3 \cdot 6H_2O$ (0.186 g, 0.5 mmol), $m$-$H_2BDC$ (0.083 g, 0.5 mmol), MOPIP (0.163 g, 0.5 mmol), NaOH (0.004 g, 0.1 mmol), and $H_2O$ (18 mL) was placed in a 25 mL Teflon-lined stainless steel vessel under autogenous pressure at 165°C for 5 days. After cooling to room temperature, red block crystals of **2** were collected by filtration and washed with distilled water (60% yield based on Ln). Anal. Calcd for **2** $C_{64}H_{40}N_8O_{15}Nd_2$ (%): C, 53.03; H, 2.79; N, 7.73. Found (%): C, 53.01; H, 2.80; N, 7.75. IR (KBr): $\acute{\upsilon} = 3071$(w), 1614(s), 1526(s), 1450(s), 1340(s), 1254(m), 1181(w), 1075(m), 739(m), 525(m), 417(m) $cm^{-1}$.

### 2.3. *Single-crystal X-ray diffraction determination*

Single-crystal X-ray data were collected at room temperature with a Rigaku Satum IICCD diffractometer equipped with graphite-monochromated Mo-Kα radiation ($\lambda = 0.71073$ Å) by using a $\varphi$–$\omega$ scan mode at 293(2) K. The structures were solved by direct methods with SHELXS-97 [10] and refined by SHELXL-97 [11] using full-matrix least-squares techniques on $F^2$. All non-hydrogen atoms were refined anisotropically and hydrogen atoms isotropically. All H atoms were positioned geometrically (C–H = 0.093 nm for CH or 0.096 nm for $CH_3$) and refined as riding. The crystal water molecules in **1** and **2** were disordered, preventing location of the hydrogen atoms in difference Fourier maps. The detailed crystallographic data and structure refinement parameters for **1** and **2** are summarized in table 1; selected bond lengths and angles are listed in tables 2 and 3.

## 3. Results and discussion

### 3.1. *Crystal structure*

Single-crystal X-ray diffraction reveals that the two compounds are isomorphous, so only the structure of **1** is described here. Each asymmetric unit contains one $Sm^{3+}$ coordinated by two nitrogen atoms from one MOPIP, six oxygen atoms from five *m*-$BDC^{2-}$, in which four μ-$O_2C$ oxygen atoms stem from four *m*-$BDC^{2-}$ ligands, and two chelating $O^-_{COO}$ come from another *m*-$BDC^{2-}$ (figure 1). There is also a disordered water molecule in the structure. The Sm–N distances are 2.580(4) and 2.599(4) Å,

Table 1. Crystallographic data and structure refinements for **1** and **2**.

| Complex | **1** | **2** |
|---|---|---|
| Empirical formula | $C_{64}H_{42}N_8O_{15}Sm_2$ | $C_{64}H_{40}N_8O_{15}Nd_2$ |
| Formula weight | 1463.76 | 1449.52 |
| Temperature (K) | 293(2) | 293(2) |
| Crystal system | Monoclinic | Monoclinic |
| Space group | *P2₁/m* | *P2₁/m* |
| Unit cell dimensions (Å, °) | | |
| *a* | 9.784(2) | 9.803(2) |
| *b* | 18.285(4) | 18.393(4) |
| *c* | 17.131(3) | 17.135(3) |
| *β* | 106.34(3) | 106.20(3) |
| Volume (Å$^3$) | 2940.9(10) | 2966.9(10) |
| *Z* | 2 | 2 |
| Calculated density (g cm$^{-3}$) | 1.653 | 1.623 |
| Absorption coefficient (mm$^{-1}$) | 2.054 | 1.807 |
| *F*(000) | 1452 | 1440 |
| Crystal size (mm$^3$) | 0.325 × 0.234 × 0.213 | 0. 355 × 0.285 × 0.263 |
| $\theta$ range for data collection (°) | 3.01–25.35 | 3.01–25.34 |
| Limiting indices | $-10 \le h \le 11$;<br>$-22 \le k \le 20$;<br>$-19 \le l \le 20$ | $-11 \le h \le 9$;<br>$-21 \le k \le 22$;<br>$-20 \le l \le 18$ |
| Reflections collected/unique | 13,828/5524 | 13,860/5562 |
| $R_{int}$ | 0.0330 | 0.0210 |
| $R_1$, $wR_2$ [$I > 2\sigma(I)$] | 0.0396, 0.1002 | 0.0346, 0.0674 |

Table 2. Selected bond lengths (Å) and angles (°) for **1**.

| | | | |
|---|---|---|---|
| Sm(1)–N(1) | 2.580(4) | Sm(1)–N(2) | 2.599(4) |
| Sm(1)–O(1) | 2.622(3) | Sm(1)–O(2) | 2.365(3) |
| Sm(1)–O(3) | 2.412(3) | Sm(1)–O(4)A | 2.317(3) |
| Sm(1)–O(5) | 2.414(3) | Sm(1)–O(6)A | 2.365(3) |
| N(1)–Sm(1)–N(2) | 63.07(12) | N(1)–Sm(1)–O(1) | 75.27(12) |
| N(1)–Sm(1)–O(2) | 83.67(13) | N(1)–Sm(1)–O(3) | 144.69(12) |
| N(1)–Sm(1)–O(4)A | 81.88(13) | N(1)–Sm(1)–O(5) | 138.32(11) |
| N(1)–Sm(1)–O(6)A | 82.27(11) | N(2)–Sm(1)–O(1) | 110.05(12) |
| N(2)–Sm(1)–O(2) | 69.10(12) | N(2)–Sm(1)–O(3) | 131.93(11) |
| N(2)–Sm(1)–O(4)A | 79.49(12) | N(2)–Sm(1)–O(5) | 76.39(11) |
| N(2)–Sm(1)–O(6)A | 140.78(11) | O(1)–Sm(1)–O(2) | 52.02(11) |
| O(1)–Sm(1)–O(3) | 69.48(11) | O(1)–Sm(1)–O(4)A | 146.74(12) |
| O(1)–Sm(1)–O(5) | 131.16(11) | O(1)–Sm(1)–O(6)A | 75.38(11) |
| O(2)–Sm(1)–O(3) | 76.46(12) | O(2)–Sm(1)–O(4)A | 148.59(12) |
| O(2)–Sm(1)–(5) | 91.02(12) | O(2)–Sm(1)–O(6)A | 127.40(11) |
| O(3)–Sm(1)–(4)A | 128.46(13) | O(3)–Sm(1)–O(5) | 71.65(11) |
| O(3)–Sm(1)–O(6)A | 86.97(11) | O(4)A–Sm(1)–O(5) | 81.67(12) |
| O(4)A–Sm(1)–O(6)A | 77.89(11) | O(5)–Sm(1)–O(6)A | 130.50(10) |

Symmetry code: A: $-x+2, -y+1, -z+1$.

Table 3. Selected bond lengths (Å) and angles (°) for **2**.

| | | | |
|---|---|---|---|
| Nd(1)–N(1) | 2.628(3) | Nd(1)–N(2) | 2.614(3) |
| Nd(1)–O(1) | 2.633(2) | Nd(1)–O(2) | 2.397(2) |
| Nd(1)–O(3) | 2.412(3) | Nd(1)–O(4) | 2.354(3) |
| Nd(1)–O(5) | 2.444(2) | Nd(1)–O(6) | 2.393(2) |
| N(1)–Nd(1)–N(2) | 62.23(9) | N(1)–Nd(1)–O(1) | 109.74(9) |
| N(1)–Nd(1)–O(2) | 69.01(9) | N(1)–Nd(1)–O(3) | 131.95(9) |
| N(1)–Nd(1)–O(4) | 79.93(9) | N(1)–Nd (1)–O(5) | 76.41(9) |
| N(1)–Nd(1)–O(6) | 139.97(9) | N(2)–Nd(1)–O(1) | 75.39(9) |
| N(2)–Nd(1)–O(2) | 82.88(10) | N(2)–Nd(1)–O(3) | 144.50(91) |
| N(2)–Nd(1)–O(4) | 82.41(10) | N(2)–Nd(1)–O(5) | 137.58(9) |
| N(2)–Nd(1)–O(6) | 82.30(9) | O(1)–Nd (1)–O(2) | 51.64(8) |
| O(1)–Nd(1)–O(3) | 69.14(8) | O(1)–Nd(1)–O(4) | 146.94(9) |
| O(1)–Nd(1)–O(5) | 131.11(8) | O(1)–Nd(1)–O(6) | 75.62(8) |
| O(2)–Nd(1)–O(3) | 76.37(9) | O(2)–Nd(1)–O(4) | 148.94 (9) |
| O(2)–Nd(1)–O(5) | 91.29(9) | O(2)–Nd(1)–O(6) | 127.23(9) |
| O(3)–Nd(1)–O(4) | 128.40(9) | O(3)–Nd(1)–O(5) | 72.04(8) |
| O(3)–Nd(1)–O(6) | 87.69(8) | O(4)–Nd(1)–O(5) | 81.51(9) |
| O(4)–Nd(1)–O(6) | 77.39(9) | O(5)–Nd(1)–O(6) | 131.12(8) |

and the Sm–O distances are 2.317(3)–2.622(3) Å. All the bond lengths are in agreement with those reported in other Sm(III) coordination polymers based on N,O-mixed ligands [7].

The six *m*-BDC$^{2-}$ ligands link dinuclear units [$Sm_2O_{12}N_4$] with an Sm1–Sm2 distance of 4.1198 Å. The dinuclear units are further linked by *m*-BDC$^{2-}$ along the *b*-axis to form a three-strand structure. The dinuclear units can be seen as octahedral secondary building units [12, 13], and in which *m*-BDC$^{2-}$ is a V-shaped linker. The *m*-BDC$^{2-}$ are arranged in a wavy fashion, with two different coordination modes and all oxygen atoms are involved in coordinating to the two Sm$^{3+}$ ions: (1) bidentate syn–syn bridging linking two adjacent units and (2) bidentate chelating with two carboxylates bridging

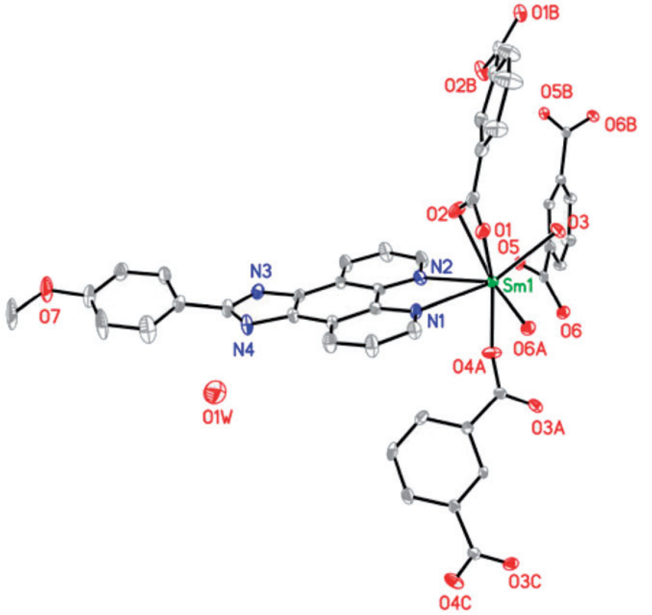

Figure 1. ORTEP drawing of **1** showing the local coordination environment of Sm(III). Thermal ellipsoids at 30% probability level.

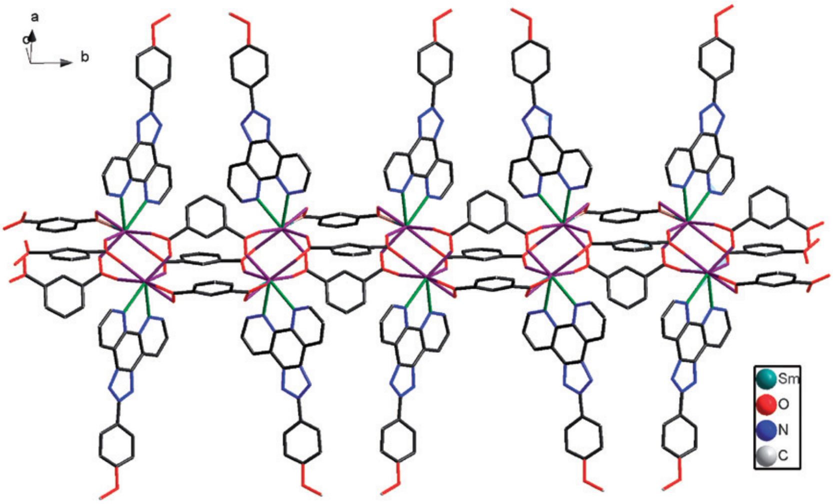

Figure 2. 1-D zipper-like chain structure of **1**.

two $Sm^{3+}$ ions of neighboring units. The MOPIP ligands are located at both sides of the ribbons, looking like a three-strand zipper, which is rare in 1-D structures and hardly appears with smaller transition metal ions (figure 2).

The three-strand zippers are further assembled into a 3-D network by $\pi \cdots \pi$ interactions. The first is offset face-to-face $\pi \cdots \pi$ stacking interaction with centroid-to-face distance of 3.6258(6) Å between imidazole rings and the terminal benzene units of

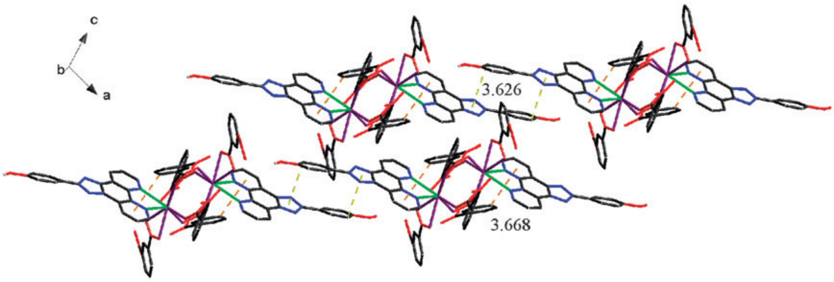

Figure 3. $\pi\cdots\pi$ stacking interactions in **1**.

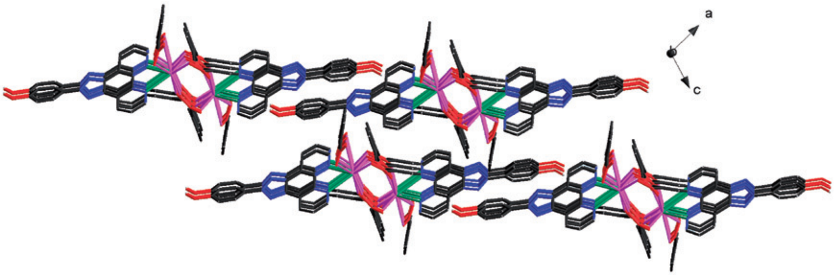

Figure 4. Perspective views of 3-D supramolecular packing structure of **1**.

MOPIP in adjacent chains. The second $\pi\cdots\pi$ stacking interactions occurs between $m$-BDC$^{2-}$ anions and phen of MOPIP in one chain in an edge-to-face fashion with a distance of 3.6680(6) Å. The $\pi\cdots\pi$ stacking interactions are shown in figure 3. Additionally, the 3-D network structure by $\pi\cdots\pi$ interactions is shown in figure 4.

### 3.2. *FT-IR analysis*

FT-IR spectra of **1** and **2** exhibit strong absorptions for the carboxylates of BDC$^{2+}$ in asymmetric and symmetric vibration regions. The asymmetric stretching vibration $\nu_{as}$(COO−) is at 1615 cm$^{-1}$ for **1** (**2**, 1614 cm$^{-1}$). The symmetric stretching vibration $\nu_s$(COO−) is observed at 1451 cm$^{-1}$ (**2**, 1450 cm$^{-1}$) [14, 15]. The difference ($\Delta = 164$ cm$^{-1}$ for **1** and **2**) between $\nu_s$(COO−) and $\nu_{as}$(COO−) is similar to that of an ionic carboxylate of BDC$^{2+}$ and less than 200 cm$^{-1}$, which indicates that all of the carboxylate groups are coordinated with metals [16]. Bands of $\nu$(C–N) (1529 cm$^{-1}$) and $\nu$(C–H) (1103 cm$^{-1}$, 827 cm$^{-1}$) of MOPIP shift to lower values at 1528, 1077, and 740 cm$^{-1}$ for **1** (1526, 1075 739 cm$^{-1}$ for **2**) in the spectra, indicating coordination of nitrogen [17]. The signal at 525 cm$^{-1}$ for **1** (525 cm$^{-1}$ for **2**) also proves coordination of metal and nitrogen. The band at 423 cm$^{-1}$ for **1** (417 cm$^{-1}$ for **2**) indicates that the metal ions are coordinated with oxygen atoms [18].

### 3.3. *Fluorescence*

The solid state luminescence spectrum for **1** excited at 361 nm is recorded at room temperature as shown in figure 5. In order to understand the nature of the emission

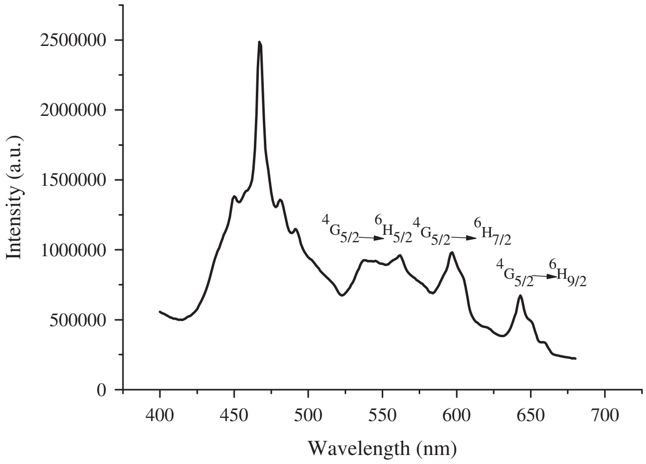

Figure 5. Fluorescent emission spectra of **1** in the solid state at room temperature.

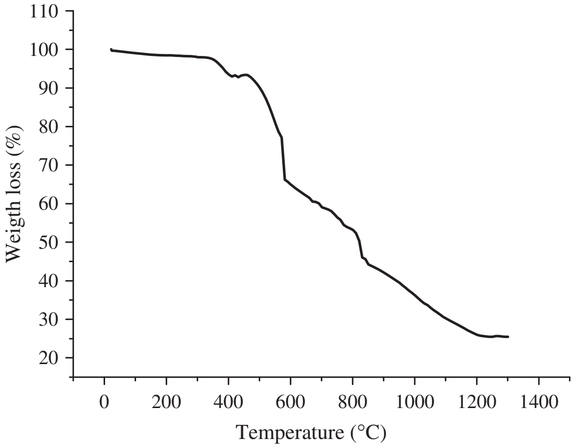

Figure 6. TG curve of **1**.

band, the luminescence of free MOPIP was observed at wavelengths of 467 nm ($\lambda_{ex} = 361$ nm), which could be attributed to the $\pi^* \rightarrow \pi$ and $\pi^* \rightarrow n$ transitions [19]. Compared to luminescence spectrum of free MOPIP, the band at 467 nm for **1** corresponds to MOPIP. Bands at 561, 598, and 644 nm belong to $^4G_{5/2} \rightarrow {}^6H_{5/2}$, $^4G_{5/2} \rightarrow {}^6H_{7/2}$, and $^4G_{5/2} \rightarrow {}^6H_{9/2}$ transitions of $Sm^{3+}$, respectively [20], suggesting that **1** will be an excellent candidate for photoluminescent material.

### 3.4. *Thermal property*

Thermal stabilities of **1** and **2** were examined using a thermogravimetric (TG) analyzer. Because of the similarity of **1** and **2**, **1** was selected as the example. From the TG curve (figure 6), **1** shows a three-step weight loss. The first of 1.96% (Calcd 1.23%) is assigned to one free water molecule which occurred at 100–254°C. The second weight loss of 31.26% (Calcd 33.63%) between 351°C and 585°C is ascribed to loss of $BDC^{2+}$. The last loss of 40.06% (Calcd 44.59%) occurs from 585°C to 1217°C, which corresponds to loss of MOPIP [21]. After decomposition, the final product may be $Sm_2O_3$ [20].

## 4. Conclusion

Lanthanide-based metal–organic frameworks constructed from polycarboxylates have been reported (e.g., $[Ln_4(BDC)_6(H_2O)_2]_n$ [Ln = Er (**1**); Tm (**2**)], $\{[Nd_2(BDC)_6(EDTA)(H_2O)_2]\cdot 1.5H_2O\}_n$, $\{[Ln(pta)(H_2O)_3]\cdot H_2O\}_n$ [Ln = Sm (**1**); Dy (**2**)] ($H_3pta$ = 2,4,6-pyridinetricarboxylic acid), and $(phen)[Ln(C_7H_3NO_5)(C_7H_4NO_5)\cdot 3H_2O]\cdot nH_2O$ [Ln = La (**1**); Pr (**2**); Nd (**3**)]) [22–24]. Coordination polymers $[Ln_2(m\text{-}BDC)_3(MOPIP)_2\cdot H_2O]_n$ [Ln = Sm (**1**), Nd (**2**)] have been synthesized from MOPIP and $H_2BDC$ under hydrothermal reaction. The aromatic carboxylate ligands adopt two different coordination modes to coordinate metals into infinite 1-D zipper-like chains, and further assembled into a 3-D network by $\pi\cdots\pi$ stacking interactions between imidazole rings and terminal benzene units of MOPIP in the adjacent chains, comparable to $(phen)[Ln(C_7H_3NO_5)(C_7H_4NO_5)\cdot 3H_2O]\cdot nH_2O$ [Ln = La (**1**); Pr (**2**); Nd (**3**)] [24]. The complexes exhibit strong fluorescence in the solid state at room temperature.

### Supplementary material

Crystallographic data for **1** and **2** have been deposited at the Cambridge Crystallographic Data Centre with the deposition numbers of CCDC 843831 and 845623. Copies of this information may be obtained free of charge from The Director, CCDC, 12 Union Road, Cambridge CB2 1EZ, UK (Fax: +44 1223 336033; E-mail: deposit@ccdc.cam.ac.uk or http://www.ccdc.cam.ac.uk) or from the corresponding author on request.

### Acknowledgments

This work is supported by the Research Fund for the Doctoral Innovative Program of Jiangsu Province (No. CXLX11_0581).

### References

[1] X.W. Wang, X. Li, J.Z. Chen, G. Zheng, H.L. Hong. *Eur. J. Inorg. Chem.*, 98 (2008).
[2] C.A. Barta, S.R. Bayly, P.W. Read, B.O. Patrick, R.C. Thompson, C. Orvig. *Inorg. Chem.*, **47**, 2280 (2008).
[3] A. de Bettencourt-Dias. *Inorg. Chem.*, **44**, 2734 (2005).

[4] F.F. Chen, Z.Q. Bian, Z.W. Liu, D.B. Nie, Z.Q. Chen, C.H. Huang. *Inorg. Chem.*, **47**, 2507 (2008).
[5] X. Li, D.Y. Wei, S.J. Huang, Y.Q. Zheng. *J. Solid State Chem.*, **182**, 95 (2009).
[6] C.C. Wang, Z.H. Wang, F.B. Gu, G.S. Guo. *J. Mol. Struct.*, **1004**, 39 (2011).
[7] H.B. Zhang, Y. Peng, X.C. Shan, C.B. Tia, P. Lin, S.W. Du. *Inorg. Chem. Commun.*, **4**, 14 (2011).
[8] Y.J. Huang, L. Ni. *Chin. J. Inorg. Chem.*, **27**, 1649 (2011).
[9] B. Liu, S. Zhou, X.M. Li, C.B. Li. *Chin. J. Struct. Chem.*, **27**, 1195 (2008).
[10] G.M. Sheldrick. *SHELXS-97, Program for the Solution of Crystal Structure*, University of Göttingen, Germany (1997).
[11] G.M. Sheldrick. *SHELXL-97, Program for the Refinement of Crystal Structure*, University of Göttingen, Germany (1997).
[12] D.J. Tranchemontagne, J.L. Mendoza-Cortes, M. O'Keeffe, O.M. Yaghi. *Chem. Soc. Rev.*, **38**, 1257 (2009).
[13] X.C. Wang, C.B. Liu, J. Chen, X.Y. Li, G.B. Che, Y.S. Yan. *Z. Anorg. Allg. Chem.*, **637**, 698 (2011).
[14] X.J. Zhang, Y.H. Xing, Z. Sun, J. Han, Y.H. Zhang, M.F. Ge, S.Y. Niu. *Cryst. Growth Des.*, **7**, 2041 (2007).
[15] G.B. Che, J. Wang, B. Liu, X.Y. Li, C.B. Liu. *J. Coord. Chem.*, **62**, 302 (2009).
[16] X. Shi, G.S. Zhu, X.H. Wang, G.H. Li, Q.R. Fang, X.J. Zhao, G. Wu, G. Tian, M. Xue, R.W. Wang, S.L. Qiu. *Cryst. Growth Des.*, **5**, 341 (2005).
[17] L. Tian, N. Ren, J.J. Zhang, H.M. Liu, J.H. Bai, H.M. Ye, S.J. Sun. *Inorg. Chim. Acta*, **362**, 3388 (2009).
[18] K. Nakamoto. *Infrared and Raman Spectra of Inorganic and Coordination Compounds*, 4th Edn, Wiley Interscience, New York (1986).
[19] W. Chen, J.Y. Wang, C. Chen, Q. Yue, H.M. Yuan, J.S. Chen, S.N. Wang. *Inorg. Chem.*, **42**, 944 (2003).
[20] X.J. Wang, Z.G. Jiang, J. Chen, Y.L. Feng. *Inorg. Chim. Acta*, **373**, 270 (2011).
[21] G.B. Che, J. Chen, X.C. Wang, C.B. Liu, C.J. Wang, S.T. Wang, Y.S. Yan. *Inorg. Chem. Commun.*, **14**, 1086 (2011).
[22] W.D. Song, J.B. Yan, H. Wang, L.L. Ji, D.Y. Ma, S.W. Ng. *J. Coord. Chem.*, **63**, 625 (2010).
[23] H.S. Wang, G.C. Li, Y. Chen, Z.J. Zhang, M.L. Liu. *J. Coord. Chem.*, **63**, 4068 (2010).
[24] J.P. Zou, M.H. Chen, M.J. Li, Q.J. Xing, A.Q. Zhang, Q. Peng. *J. Coord. Chem.*, **63**, 3576 (2010).